Electronic supplementary materials *Mendeleev Commun.*, 2025, **35**, 145–147

New thiosemicarbazones possessing activity against SARS-CoV-2 and H1N1 influenza viruses

Olga A. Zhupikova, Olga I. Yarovaya, Mariya K. Marenina, Yulia V. Meshkova, Svetlana V. Belenkaya, Dmitriy N. Shcherbakov, Anna V. Zaykovskaya, Oleg V. Pyankov, Vladimir V. Zarubaev, Mikhail G. Mikhalsky, Alexey Yu. Fedorov, Sergey G. Arkhipov, Vladimir I. Potkin, Irina A. Kolesnik, Andrey V. Ivanov, Nariman F. Salakhutdinov and Mikhail V. Khvostov

Contents

General

^{1}H NMR and ^{13}C NMR spectra were obtained on Bruker AV-300 (300 MHz), AV-400 (400 MHz) and Bruker DRX-500 (100 MHz) spectrometers, respectively. The chemical shifts are given in a low field from TMS and were reported in ppm relative to residual DMSO-*d*$_6$ (δ_H=2.5, δ_C=39.5). The composition of the compounds was determined by HR-MS analysis on a Thermo Electron Corporation Double Focusing System (DFS) high resolution mass-spectrometer (direct inlet, electron ionization is 70 eV). IR spectra were obtained on a Bruker Vector-22 spectrometer. UV spectra were obtained on spectrophotometer HP/Agilent UV-Vis 8453A DAD. As starting compounds were taken 5-phenylisoxazole-3-carbaldehyde, 5-(*p*-tolyl)isoxazole-3-carbaldehyde, 5-(4-methoxyphenyl)-1*H*-pyrrole-2-carbaldehyde, 4,5,6,7-tetrahydro-1*H*-indole-2-carbaldehyde and 4,5-dihydro-1*H*-benzo[*g*]indole-2-carbaldehyde. The Synthesis of aldehydes has been described previously.[S1,S2,S3]

General synthetic procedure for compounds 1a-e

The corresponding aldehyde and thiosemicarbazide were dissolved in ethanol (50 ml) in a molar ratio of 1:3, and a few drops of HCl were added. The reaction mixture was heated for 6 h and then filtered under reduced pressure, washing with 50 ml of saturated NaCl solution and then with 50 ml of water.

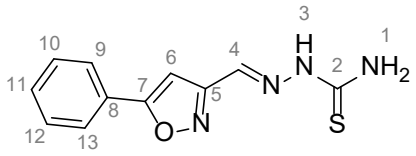

(*E*)-2-[(5-Phenylisoxazol-3-yl)methylene]hydrazine-1-carbothioamide (1a):

350.0 mg (2.0 mmol) of the corresponding aldehyde was taken. The product yield 90%, white powder, mp 169 °C with decomposition. ^{1}H NMR (DMSO-*d*$_6$, 400 MHz) δ: 11.80 (s, 1H, *H3*), 8.52 (br. s., 1H, *H4*), 8.12 (c, 2H, *H1*), 7.83 (d, *J*=7.12 Hz, 2H, *H9*, *H13*), 7.46-7.66 (m, 4H, *H6*, *H10*, *H11*, *H12*). ^{13}C NMR (DMSO-*d*$_6$, 100 MHz) δ: 178.78 (*C2*), 168.93 (*C7*), 161.14 (*C5*), 130.92 (*C4*), 130.47 (*C11*), 129.20 (*C10*, *C12*), 126.46 (*C8*), 125.36 (*C9*, *C13*), 97.68 (*C6*). IR spectra (KBr) ν, cm^{-1}: 3403, 3267, 3168, 2985, 1597, 1436, 1337. HR-MS, m/z: calculated for $C_{11}H_{10}O_1N_4S_1$ [M^+] 246.0570; found 246.0568. UV spectra: λ_{max}/nm (lgε), EtOH: 204 (4.35), 259 (4.26), 304 (4.46).

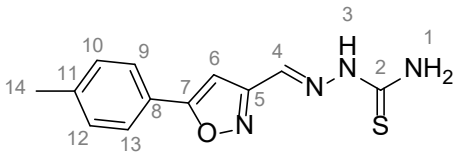

(*E*)-2-{[5-(*p*-Tolyl)isoxazol-3-yl]methylene}hydrazine-1-carbothioamide (1b):

350.0 mg (1.9 mmol) of the corresponding aldehyde was taken. The product yield 94%, light-yellow powder, mp 202–207 °C. ^{1}H NMR (DMSO-*d*$_6$, 300 MHz) δ: 11.83 (s, 1H, *H3*), 8.55 (br. s., 1H, *H4*), 8.06-8.21 (m, 2H, *H1*), 7.71 (d, *J*=7.87 Hz, 2H, *H9*, *H13*), 7.58 (s, 1H, *H6*), 7.37 (d, *J*=7.87 Hz, 2H, *H10*, *H12*), 2.37 (s, 3H, *H14*). ^{13}C NMR (DMSO-*d*$_6$, 100 MHz) δ: 178.68 (*C2*), 169.12 (*C7*), 161.29 (*C5*), 140.59 (*C11*), 130.97 (*C4*),

129.92 (*C9*, *C13*), 125.41 (*C10*, *C12*), 123.89 (*C8*), 97.23 (*C6*), 21.00 (*C14*). IR spectra (KBr) ν, cm^{-1}: 3433, 3272, 3161, 3029, 1604, 1506, 1278. HR-MS, m/z: calculated for $C_{12}H_{12}O_1N_4S_1$ [M^+] m/z=260.0726; found m/z=260.0723. UV spectra: λ_{max}/nm (lgε), EtOH: 202 (4.28), 260 (4.01), 304 (4.21).

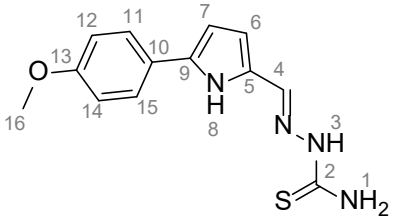

(*E*)-2-{[5-(4-Methoxyphenyl)-1*H*-pyrrol-2-yl]-methylene}hydrazine-1-carbothioamide (1c):

100.0 mg (0.5 mmol) of the corresponding aldehyde was taken. The product yield 82%, violet powder, mp 176 °C with decomposition. ^{1}H NMR (DMSO-d_6, 400 MHz) δ: 11.15-11.32 (m, 2H, *H8*, *H3*), 8.14 (d, *J*=13.16 Hz, 2H, *H1*), 7.78-7.86 (m, 1H, *H4*) 7.66 (d, *J*=8.60 Hz, 2H, *H11*, *H15*), 6.98 (d, *J*=8.60 Hz, 2H, *H12*, *H14*) 6.46 (d, *J*=1.48 Hz, 2H, *H6*, *H7*) 3.69-3.81 (m, 3H, *H16*). ^{13}C NMR (DMSO-d_6, 100 MHz) δ: 177.05 (*C2*), 158.33 (*C13*), 135.32 (*C4*), 133.53 (*C5*), 128.30 (*C9*), 125.95 (*C11*, *C15*), 124.64 (*C10*), 114.88 (*C6*), 114.23 (*C12*, *C14*), 106.69 (*C7*), 55.19 (*C16*). IR spectra (KBr) ν, cm^{-1}: 3429, 3273, 3173, 2972, 1604, 1506, 1278. HR-MS, m/z: calculated for $C_{13}H_{14}O_1N_4S_1$ [M^+] m/z=274.0676; found m/z=274.0889. UV spectra: λ_{max}/nm (lgε), EtOH: 202 (4.21), 260 (3.88), 368 (4.34), 513 (3.17).

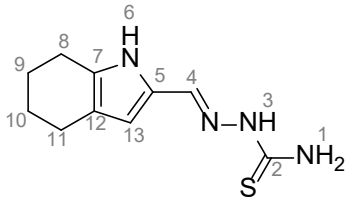

(*E*)-2-[(4,5,6,7-Tetrahydro-1*H*-indol-2-yl)methylene]hydrazine-1-carbothioamide (1d):

300.0 mg (2.0 mmol) of the corresponding aldehyde was taken. The product yield 89%, orange powder, mp 201-204 °C. ^{1}H NMR (DMSO-d_6, 300 MHz) δ: 10.29 (s, 1H, *H6*), 9.98 (br. s., 1H, *H3*), 6.96-7.17 (br. s., 2H, *H1*), 6.85 (s, 1H, *H4*), 5.24 (s, 1H, *H13*), 1.61-1.76 (m, 2H, *H8*), 1.47-1.57 (m, 2H, *H11*), 0.73-0.93 (m, 4H, *H9*, *H10*). ^{13}C NMR (DMSO-d_6, 100 MHz) δ: 176.78 (*C2*), 133.86 (*C4*), 131.43 (*C7*), 125.65 (*C5*), 117.69 (*C12*), 112.19 (*C13*), 23.30 (*C8*), 22.76 (*C11*), 22.47 (*C9*, *C10*). IR spectra (KBr) ν, cm^{-1}: 3503 (NH), 3296, 3273 (N–N), 3503, 3296, 3124, 2927, 1532 (NH), 1313. HR-MS, m/z: calculated for $C_{10}H_{14}N_4S_1$ [M^+] m/z=222.0934; found m/z=222.0935. UV spectra: λ_{max}/nm (lgε), EtOH: 203 (4.21), 246 (4.31), 272 (4.28), 348 (4.57).

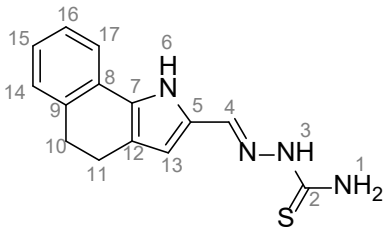

(*E*)-2-[(4,5-Dihydro-3*H*-benzo[*g*]indol-2-yl)-methylene]hydrazine-1-carbothioamide (1e):

100.0 mg (0.5 mmol) of the corresponding aldehyde was taken. The product yield 93%, green powder, mp 209-212 °C. ^{1}H NMR (DMSO-d_6, 400 MHz) δ: 11.29-11.34(m, 2H, *H3*, *H6*), 8.06-8.19 (m, 2H, *H1*, *H3*), 7.82 (s, 1H, *H4*), 7.59 (d, *J*=7.66 Hz, *H17*), 7.19-7.26 (m, 2H, *H15*, *H16*), 7.06-7.11 (m, 1H, *H14*), 6.34 (d, *J*=2.02 Hz, 1H, *H13*), 2.81-2.87 (m, 2H, *H10*), 2.59-2.66 (m, *J*=8.06 Hz, 2H, *H11*). ^{13}C NMR (DMSO-d_6, 100 MHz) δ: 177.03 (*C2*), 135.07(*C8*), 133.45 (*C4*),

130.83 (*C9*), 128.55 (*C12*), 128.23 (*C17*), 128.20 (*C7*), 126.50 (*C14*), 125.84 (*C16*), 120.88 (*C5*), 120.29(*C15*), 112.41 (*C13*), 29.16 (*C10*), 21.13 (*C11*). IR spectra (KBr) ν, cm^{-1}: 3455, 3378, 3147, 2932, 1612, 1539, 1285. HR-MS, m/z: calculated for $C_{14}H_{13}N_4S_1$ $[M^+]$ m/z=270.0934; found m/z=270.0932. UV spectra: λ_{max}/nm (lgε), EtOH: 201 (4.38), 244 (4.09), 276 (4.00), 378 (4.56), 514 (3.67).

Crystal Data

Crystal Data for **1d**. $C_{10}H_{14}N_4S$ (*M* = 222.31), monoclinic, space group *C2/c*, *a* = 13.8705(10) Å, *b* = 8.5289(4) Å, *c* = 19.6159(11) Å, *β* = 107.355(7)°, *V* = 2214.9(2) $Å^3$, *Z* = 8, *T* = 296(2) K, μ(MoKα) = 0.265 mm^{-1}, D_{calc} = 1.333 g/cm^3, 14007 reflections measured (4.35° ≤ 2Θ ≤ 52.744°), 2266 unique (R_{int} = 0.0553, R_{sigma} = 0.0350) which were used in all calculations. The final R_1 was 0.0340 (I > 2σ(I)) and wR_2 was 0.1014 (all data).

A single crystal was obtained by slow evaporation of a saturated solution of **1d** in ethanol at 296(2) K. Single-crystal X-ray diffraction data were collected at 296(2) K using a TD-5000 diffractometer [Mo-Kα radiation (λ = 0.71073 Å)] and a hybrid photon-counting detector. The investigations were performed using large-scale research facilities "EXAFS spectroscopy beamline" at the Siberian synchrotron and terahertz radiation center. Data reduction was performed using the CrysAlisPro software.[S4] The crystal structure was solved with the SHELXT[S5] program using intrinsic phasing and refined with the SHELXL[S6] refinement package using least squares minimisation with the Olex2 version 1.5 as a GUI.[S7] All non-hydrogen atoms were refined anisotropically. The hydrogen atoms bonded to carbon atoms were placed in calculated positions and refined using a riding model with fixed isotropic displacement parameters [U_{iso}(H) = 1.2U_{eq}(C)]. The hydrogen atoms bonded to N1, N2, and N4 atoms were located from the Fourier difference map and refined isotropically without additional restraints. The disordered C7A, C7B and C8A, C8B atoms with the corresponding hydrogens were refined with SADI restraints.

CCDC 2372012 contains the supplementary crystallographic data for this paper. These data can be obtained free of charge from The Cambridge Crystallographic Data Centre via http://www.ccdc.cam.ac.uk.

Table S1. Experimental details

	1d
Crystal data	
Chemical formula	$C_{10}H_{14}N_4S$
M_r	222.31
Crystal system, space group	Monoclinic, *C*2/*c*
Temperature (K)	296
a, *b*, *c* (Å)	13.8705 (10), 8.5289 (4), 19.6159 (11)
b (°)	107.355 (7)
V (Å^3)	2214.9 (2)
Z	8
Radiation type	Mo *K*a
m (mm^{-1})	0.27
Crystal size (mm)	0.4 × 0.2 × 0.05
Data collection	
Diffractometer	TD-5000 diffractometer [Mo-Kα radiation (λ = 0.71073 Å)] and a hybrid photon-counting detector
Absorption correction	Multi-scan *CrysAlis PRO* 1.171.43.90 (Rigaku Oxford Diffraction, 2023) Empirical absorption correction using spherical harmonics, implemented in SCALE3 ABSPACK scaling algorithm.
T_{min}, T_{max}	0.523, 1.000
No. of measured, independent and observed [I > 2s(I)] reflections	14007, 2266, 2061
R_{int}	0.055
(sin q/l)$_{max}$ (Å^{-1})	0.625
Refinement	
$R[F^2 > 2s(F^2)]$, $wR(F^2)$, S	0.034, 0.101, 1.08
No. of reflections	2266
No. of parameters	171
No. of restraints	2
H-atom treatment	H atoms treated by a mixture of independent and constrained refinement
$\Delta\rho_{max}$, $\Delta\rho_{min}$ (e Å^{-3})	0.18, -0.19

Biological experiments

3Clpro inhibition assay.

The preparation of the main SARS-CoV-2 protease, 3CLpro, was carried out in a previously obtained transformant *E. coli* strain, which ensures the synthesis of the target protein in soluble form. The standard cultivation protocol included the addition of the inducer IPTG. The purification of 3CLpro included cell biomass lysis and ultrasonic disintegration, as well as the purification of the clarified lysate on Ni-Sepharose.[S8] The purity of the resulting sample of 3CLpro, was assessed by SDS-PAGE under denaturing conditions according to the Laemmli method. Protein concentration was determined by the Bradford assay.[S9]

To evaluate the new thiosemicarbazones ability to inhibit 3CLpro, a semi-inhibitory concentration (IC_{50}) was used. It was calculated as concentration which reduced the fluorescence level by 50% compared to the value obtained without the addition of the inhibitor. Fluorescence was observed by an assay involving a synthetic fluorescently labeled peptide substrate of the type DabcylKTSAVLQ↓SGFRKME(Edans)NH2 (more than 95% purity, CPC Scientific Inc., Hangzhou, China) containing the site digested by 3CLpro. The signal was recorded on a SuperMax 3100 fluorimeter ("Flash", Shanghai, China) at 355 and 460 nm for excitation/emission, respectively, in kinetic scan mode. Reaction mixtures containing Tris-HCl buffer (supplemented with EDTA, NaCl; pH=7.3), 3CLpro (300 nM) and the tested compound (from 200 to 0 μM) were prepared and incubated for 30 min in a 384-well plate at 30°C, then the reaction was triggered by the addition of fluorogenic substrate (10 μM). The inhibitors of 3CLpro (Nirmatrelvir (LEAPChem, China), Disulfiram, Ebselen, GC376) were used as a positive control. IC_{50} values were calculated using the 4PL function.

Evaluation of antiviral activity against influenza virus

Viruses and cells. We used MDCK cells (ATCC CCL-34) from the collection of cell lines of the Saint Petersburg Pasteur Institute. Cells were cultured in 96-well culture plates in in Eagle's minimal essential medium (alpha-MEM) with 10% fetal bovine serum («HyClone», USA), 40 U/ml gentamicin sulfate and 2.5 U/ml amphotericin B. Cell suspension with a concentration of 10^5 cells/ml was placed in the wells of the plates in volume of 100 μl and cultured until a complete monolayer formation for 24 h at 36 °C in the presence of 5% CO_2.

The same medium without serum was used as a support medium for culturing cells with viruses.

We used influenza virus A/Puerto Rico/8/34 (H1N1) from the collection of the Saint Petersburg Pasteur Institute. The infectious titers of the virus were determined by titration in 96-well plates with monolayers of MDCK cells. The results were evaluated visually according to the presence of the virus cytopathic effect (CPE), the virus titer was calculated by Reed and Muench method and represented as decimal logarithms of 50% tissue culture infectious doses per ml (lg $TCID_{50}$/ml).

Cytotoxicity assay. The microtetrazolium test (MTT) was used to study the cytotoxicity of the compounds. Briefly, a series of three-fold dilutions of each compound (300–3.7 μg mL−1) alpha-MEM were prepared. MDCK cells were incubated for 48 h at 36 °C in 5% CO2 in the presence of the dissolved substances. The cells were washed twice with phosphate-buffered saline (PBS), and a solution of 3-(4,5-dimethylthiazolyl-2)-2,5-diphenyltetrazolium bromide (ICN Biochemicals Inc. Aurora, Ohio) (0.5 mg mL^{-1}) in PBS was added to the wells. After 1 h incubation, the wells were washed and the formazan residue was dissolved in DMSO (0.1 mL per well). The optical density in the wells was then measured using a Multiscan FC plate analyzer (Thermo Scientific) at a wavelength of 540 nm and plotted against the concentration of the compounds. Each concentration was tested in three parallels. The 50% cytotoxic concentration (CC_{50}) of each compound was calculated from the data obtained.

CPE reduction assay. The compounds in appropriate concentrations were added to MDCK cells (0.1 ml per well). After 1 h of incubation, cells were infected with influenza virus A/Puerto Rico/8/34 (H1N1) (moi 0.01) and incubated for 48 h at 36 °C and 5% CO_2. After that, cell viability was assessed by MTT test as described above. The cytoprotective activity of compounds was considered as their ability to increase the values of OD comparing to control wells (with virus only, no drugs). Based on the results obtained, the values of IC_{50}, *i.e.* concentration of compounds that result in 50% cells protection were calculated using GraphPad Prism 6.01 software. Values of IC_{50} obtained in μg/ml were then calculated into micromoles (μM). For each compound the value of selectivity index (SI) was calculated as ratio of CC_{50} to IC_{50}. Compounds with SI of 10 and higher were considered active. Rimantadine (α-methyl-1-adamantane methylamine hydrochloride) used as a reference compounds.

Evaluation of the Antiviral Activities Against SARS-CoV-2 Viruses

The SARS-CoV-2 in vitro experiment was conducted in laboratories at Biosafety Level 3 (BSL-3). It was carried out using a strain of the virus Wuhan, lineages B.1.1: hCoV-19/Russia/Omsk202118_1707/2020 (GISAID ID: EPI_ISL_1242008) (the State Collection of Pathogens of Viral Infections and Rickettsioses at the State Research Center of Virology and Biotechnology VECTOR, Rospotrebnadzor, Russia).

The viruses were propagated in cultured Vero E6 cells. These cells were grown in 96-well culture plates to a confluence of at least 95%. Samples of compounds were dissolved in dimethyl sulfoxide (DMSO) to a concentration of 10 mg/mL. Remdesivir served as a control drug. Half-maximal effective concentrations (EC_{50}) of compounds were evaluated in an assay of reduction of the cytopathic effect on cells. Serial three-fold dilutions of the compounds were prepared, starting at 600 μg/mL. To test each compound, virus doses of 100 $TCID_{50}$ (50% tissue culture infectious doses) per well were applied.

The inhibitory activities and toxicity of the tested compounds were assessed simultaneously. Specifically, dilutions of the compounds were added into the wells in the culture plates containing a monolayer of the cells. A plain medium (to determine the toxic concentration of the tested compounds) or a medium containing a virus (to determine inhibitory activities) was then added. The culture plates were incubated at 37 °C for 4 days. An MTT (3-(4,5-dimethylthiazol-2-yl)-2,5-diphenyltetrazolium bromide) (NeoFroxx) 0.5 mg/mL solution was prepared in sterile phosphate-buffered saline, and 100 μL was then added into each well and incubated at 37 °C for 4 h. Next, the supernatant from each well was carefully removed by aspiration without disturbing the cells. Then, 100 μL of DMSO was added to each well to dissolve formazan crystals. The optical density was measured on a microplate reader (ThermoScientific Multiskan FC) at 570 nm. Data processing was carried out in the SOFTmax PRO 4.0 software by a 4-parameter method. Half-maximal cytotoxic concentration (CC_{50}) and half-maximal effective concentration (EC_{50}) were both determined.

References

S1. I. A. Kolesnik, S. K. Petkevich, D. F. Mertsalov, L. V. Chervyakova, M. A. Nadirova, A. P. Tyurin, A. Y. Guan, C. L. Liu and V. I. Potkin, *Russ. J. Gen. Chem.*, 2022, **92**, 29; https://doi.org/10.1134/S1070363222010066.

S2. N. A. Bumagin, A. V. Kletskov, S. K. Petkevich, I. A. Kolesnik, A. S. Lyakhov, L. S. Ivashkevich, A. V. Baranovsky, P. V. Kurman and V. I. Potkin, *Tetrahedron*, 2018, **74**, 3578; https://doi.org/10.1016/j.tet.2018.05.016.

S3. A. I. Mikhaleva, A. B. Zaitsev, A. V. Ivanov, E. Yu. Schmidt, A. M. Vasil'tsov and B. A. Trofimov, *Tetrahedron Lett.*, 2006, **47**, 3693; https://doi.org/10.1016/j.tetlet.2006.03.126.

S4. *CrysAlis^{Pro} Software System, Version 1.171.43.90*, Rigaku Oxford Diffraction, Wroclaw, Poland, 2024.

S5. G. M. Sheldrick, *Acta Crystallogr., Sect. A: Found. Adv.*, 2015, **71**, 3; https:/doi.org/10.1107/S2053273314026370.

S6. G. M. Sheldrick, *Acta Crystallogr., Sect. C: Struct. Chem.*, 2015, **71**, 3; https://doi.org/10.1107/S2053229614024218.

S7. O. V. Dolomanov, L. J. Bourhis, R. J. Gildea, J. A. K. Howard and H. Puschmann, *J. Appl. Crystallogr.*, 2009, **42**, 339; https://doi.org/10.1107/S0021889808042726.

S8. S. V. Belenkaya, Iu. A. Merkuleva, O. I. Yarovaya,V. Yu. Chirkova, E. A. Sharlaeva, D. V. Shanshin, E. A. Volosnikova, S. Z. Vatsadze, M. V. Khvostov, N. F. Salakhutdinov and D. N. Shcherbakov, *Front. Bioeng. Biotechnol.*, 2023, **11**, 1187761; https://doi.org/10.3389/fbioe.2023.1187761.

S9. M. M. Bradford, *Anal. Biochem.*, 1976, **72**, 248; https://doi.org/10.1006/abio.1976.9999.

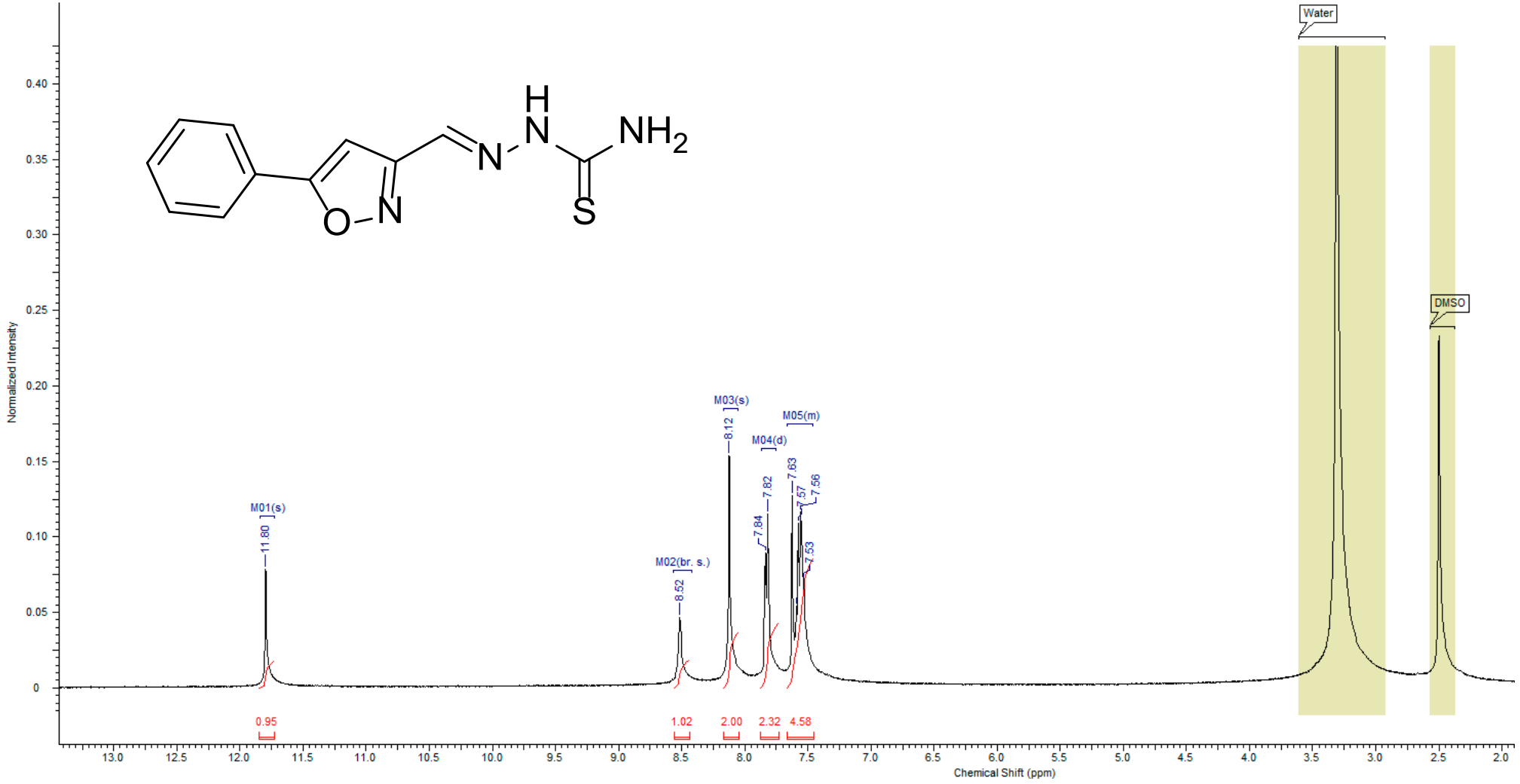

Figure S1. ^{1}H NMR spectrum of compound **3a** in DMSO-d_6 at 400 MHz

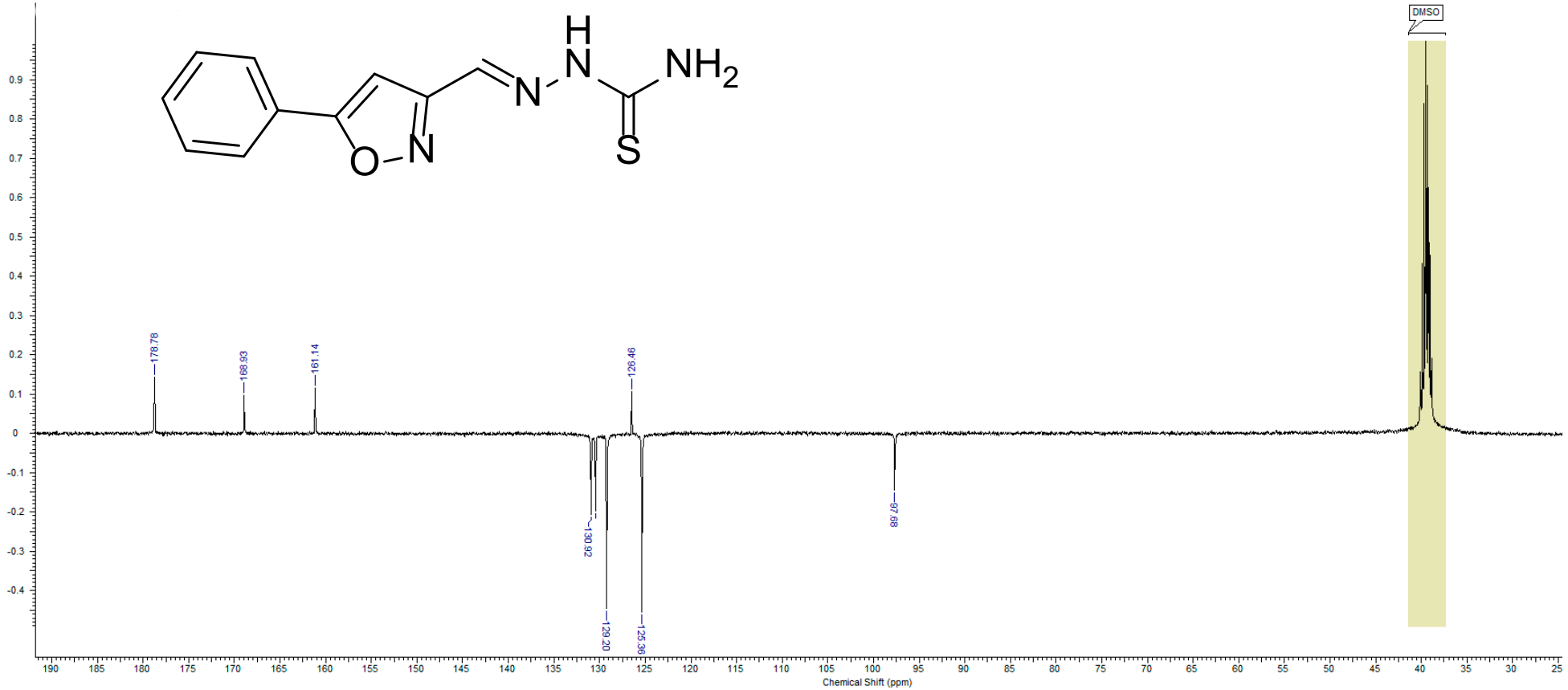

Figure S2. ^{13}C NMR spectrum of compound **3a** in DMSO-d_6 at 100 MHz

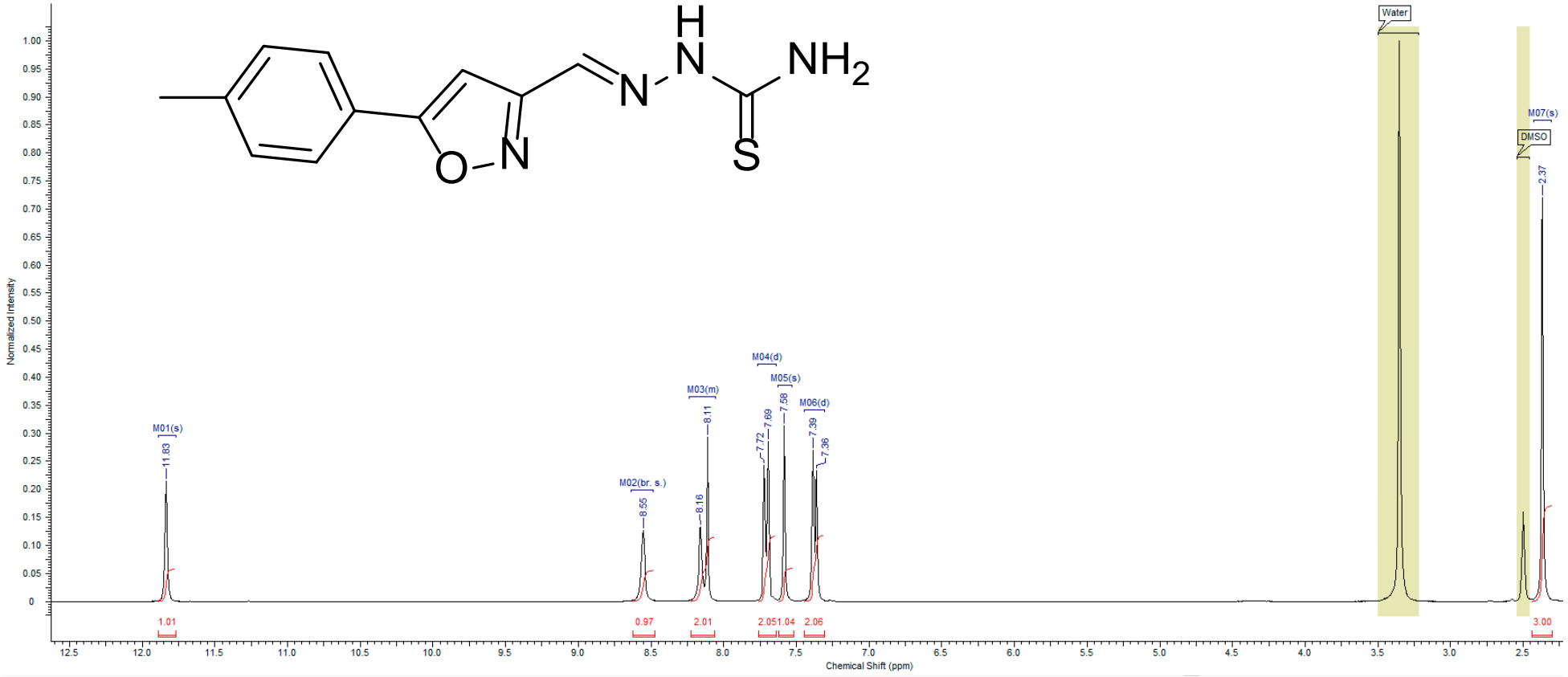

Figure S3. ^{1}H NMR spectrum of compound **3b** in DMSO-d_6 at 300 MHz

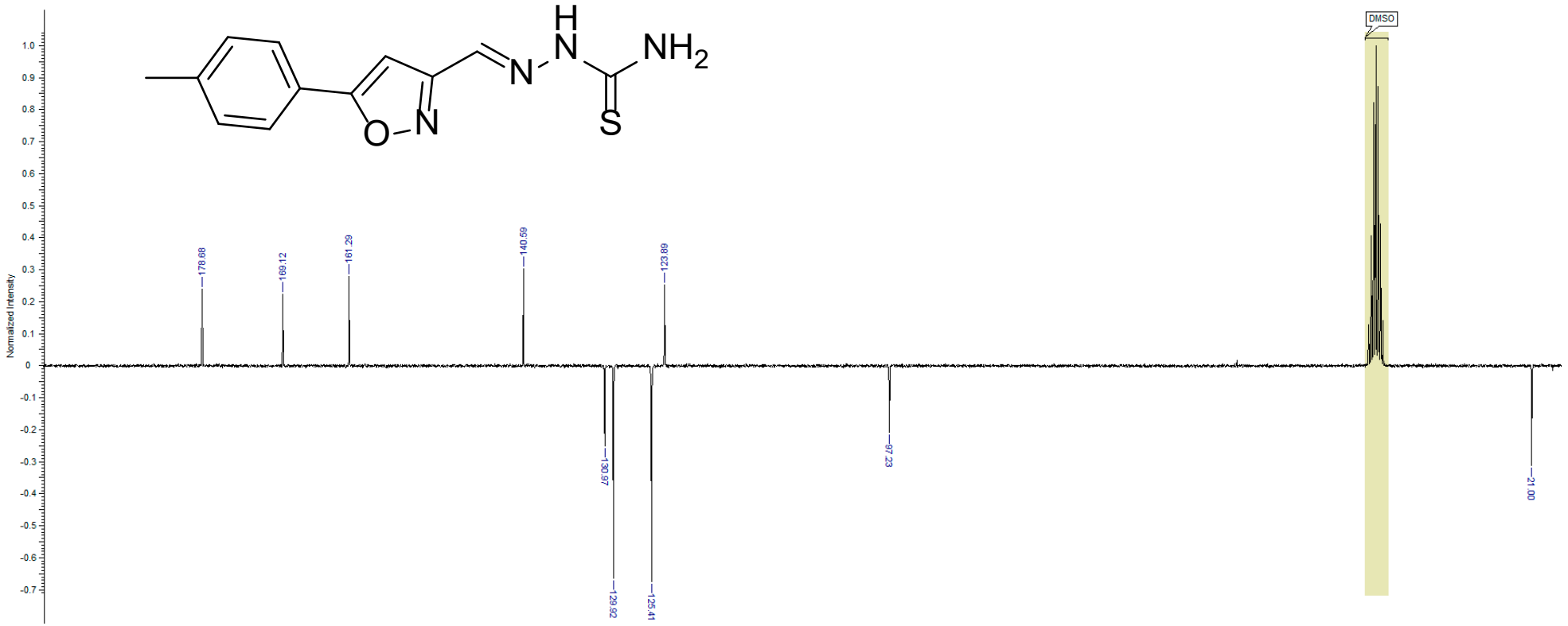

Figure S4. ^{13}C NMR spectrum of compound **3b** in DMSO-d_6 at 100 MHz

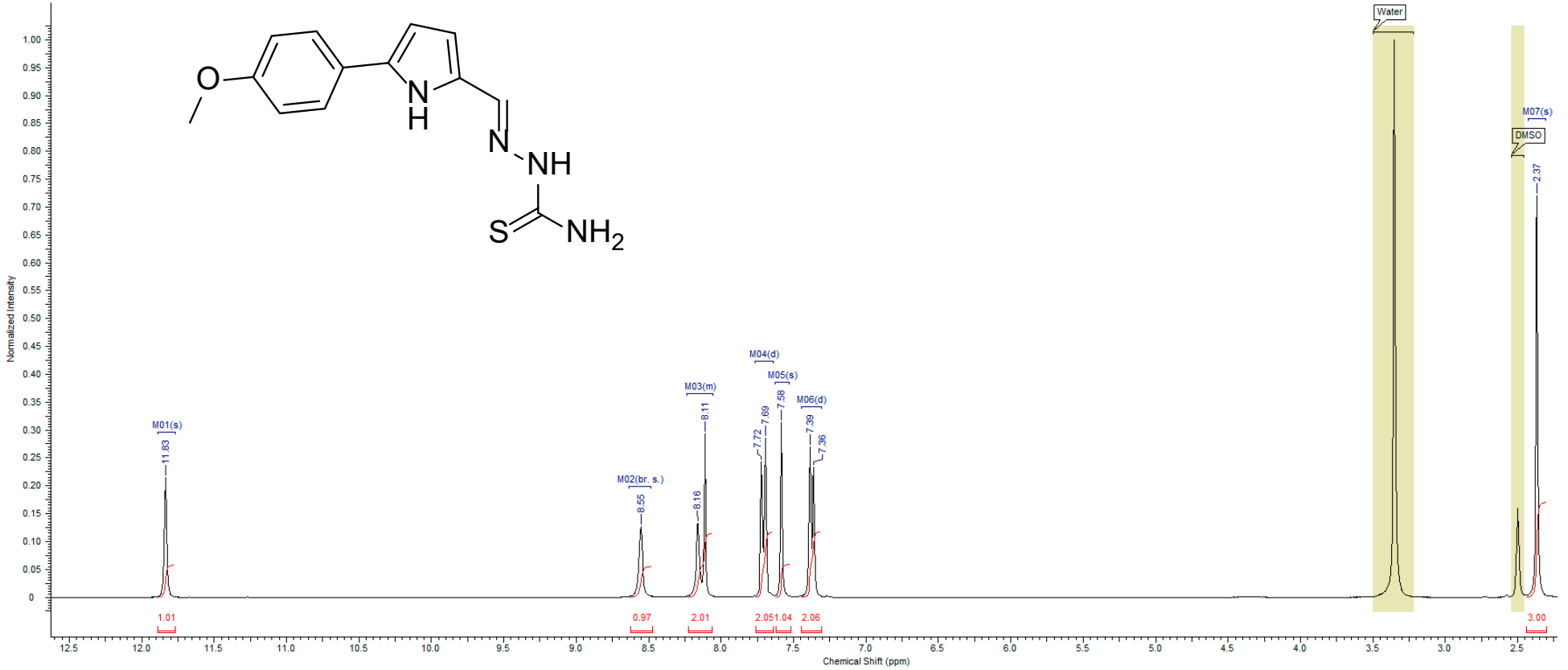

Figure S5. ^{1}H NMR spectrum of compound **3c** in DMSO-d_6 at 400 MHz

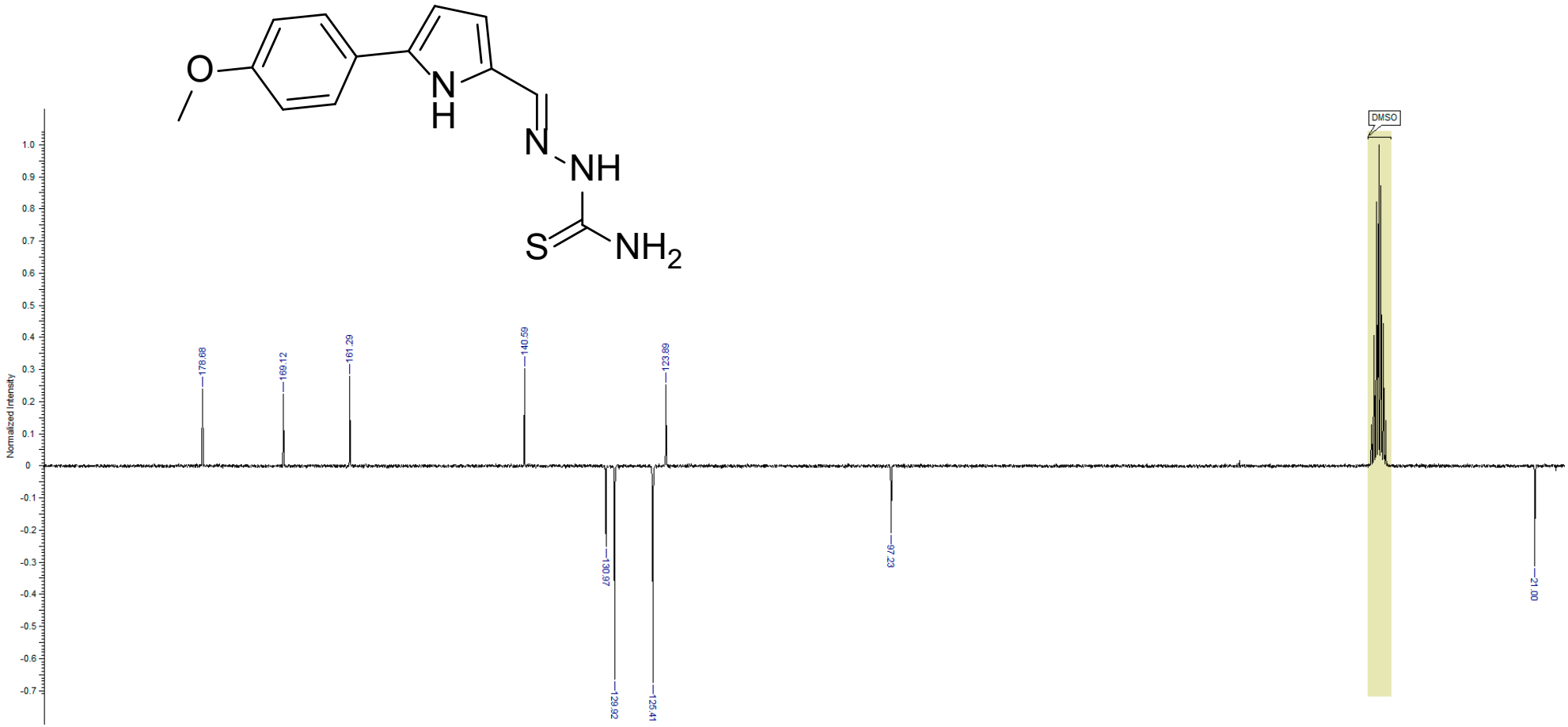

Figure S6. ^{13}C NMR spectrum of compound **3c** in DMSO-d_6 at 100 MHz

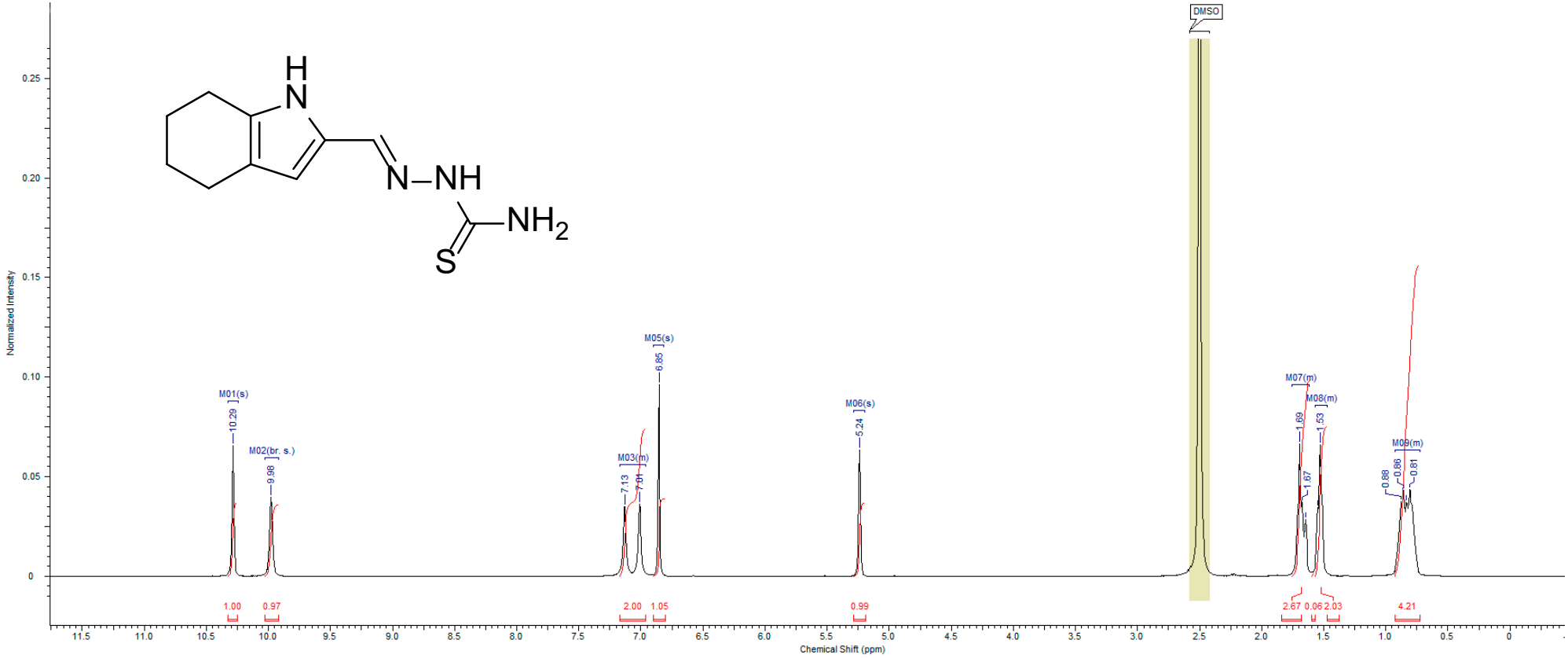

Figure S7. ^{1}H NMR spectrum of compound **3d** in DMSO-d_6 at 300 MHz

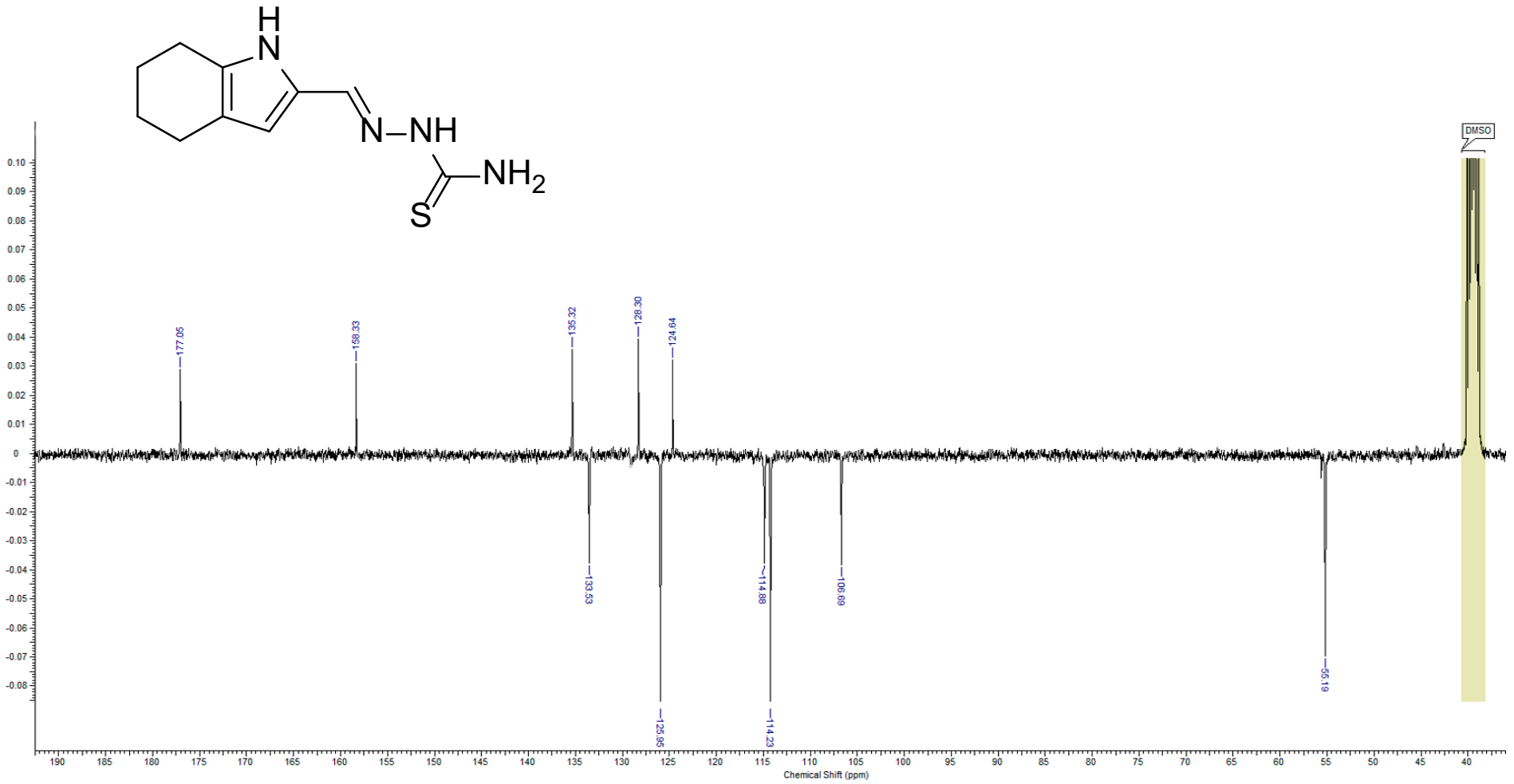

Figure S8. ^{13}C NMR spectrum of compound **3d** in DMSO-d_6 at 100 MHz

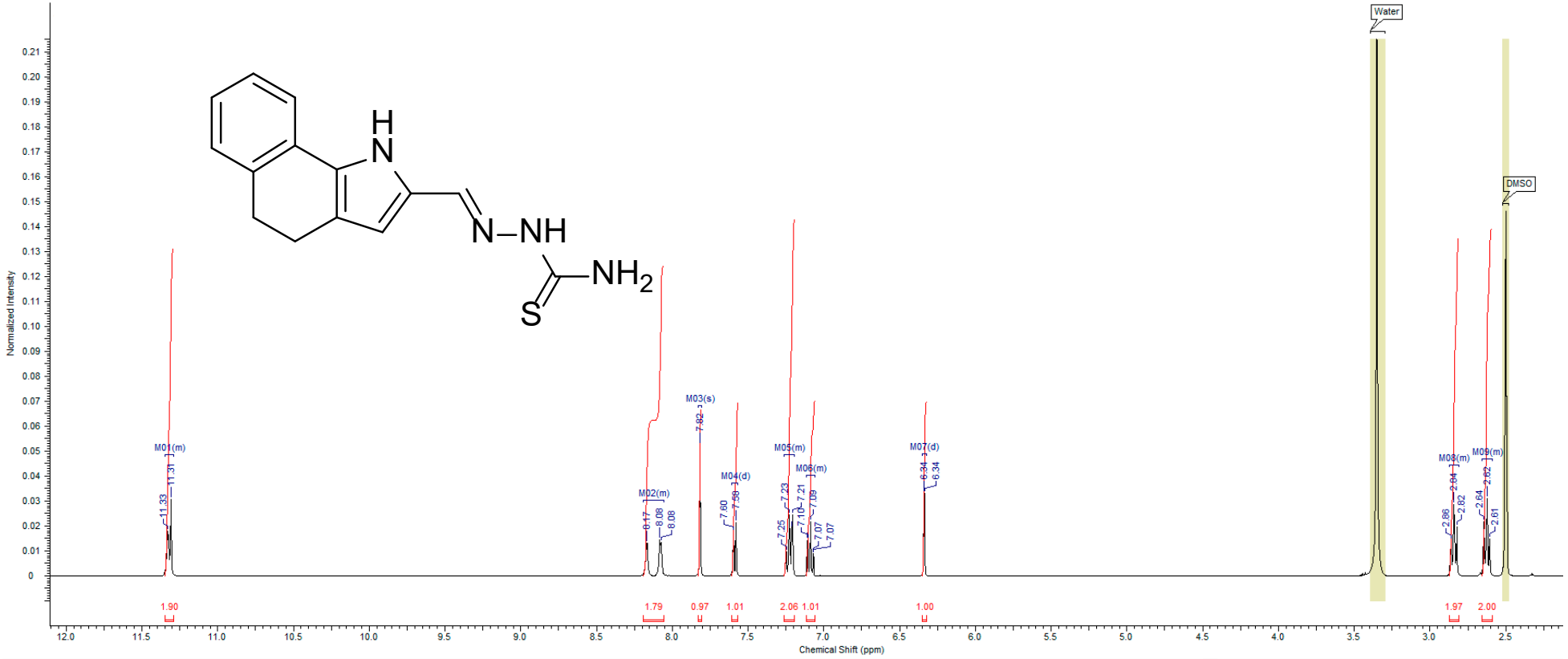

Figure S9. ^{1}H NMR spectrum of compound **3f** in DMSO-d_6 at 400 MHz

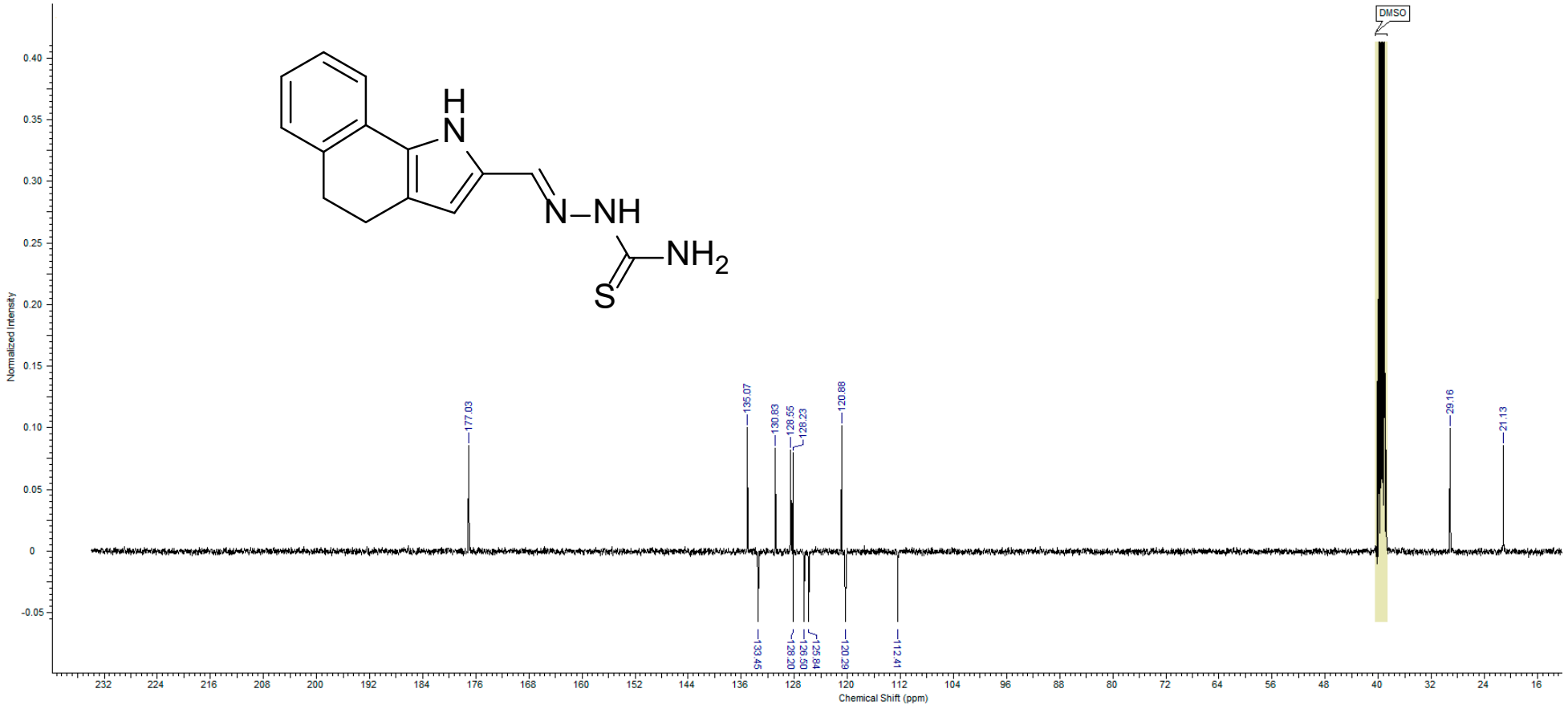

Figure S10. ^{13}C NMR spectrum of compound **3f** in DMSO-d_6 at 100 MHz